# Stabilization of the Resistive Wall Mode by Magnetic Feedback and Plasma Rotation

Y.Q. Liu[1], A. Bondeson[1], D. Gregoratto[1],

C.M. Fransson[2], B. Lennartson[2], C. Breitholtz[2], Y. Gribov[3]

with contributions from

M.S. Chu[4], R. La Haye[4], A. Garofalo[5], T. Hender[6], M. Gryaznevich[6],

A. Polevoi[3], V.D. Pustovitov[7]

[1]*Department of Electromagnetics, EURATOM-VR/Fusion Association*

[2]*Department of Signals and Systems*

*Chalmers University of Technology, Gothenburg, Sweden*

[3]*Physics Unit, ITER Naka Joint Work Site, Naka, Ibaraki, Japan*

[4]*General Atomics, San Diego, USA*

[5]*Columbia University, New York, USA*

[6]*UKAEA/Euratom Fusion Association, Culham, UK*

[7]*Russian Research Centre Kurchatov Institute, Moscow, Russia*

**Workshop on Active Control of MHD Stability: Extension to the Burning Plasma Regime**

**University of Texas-Austin, Austin, Texas, USA, November 3-5, 2003**

# Outline

- **Feedback**
- **Rotation**
- **Feedback $+$ Rotation**
- **Resonant Field Amplification (RFA)**
- **Conclusions**

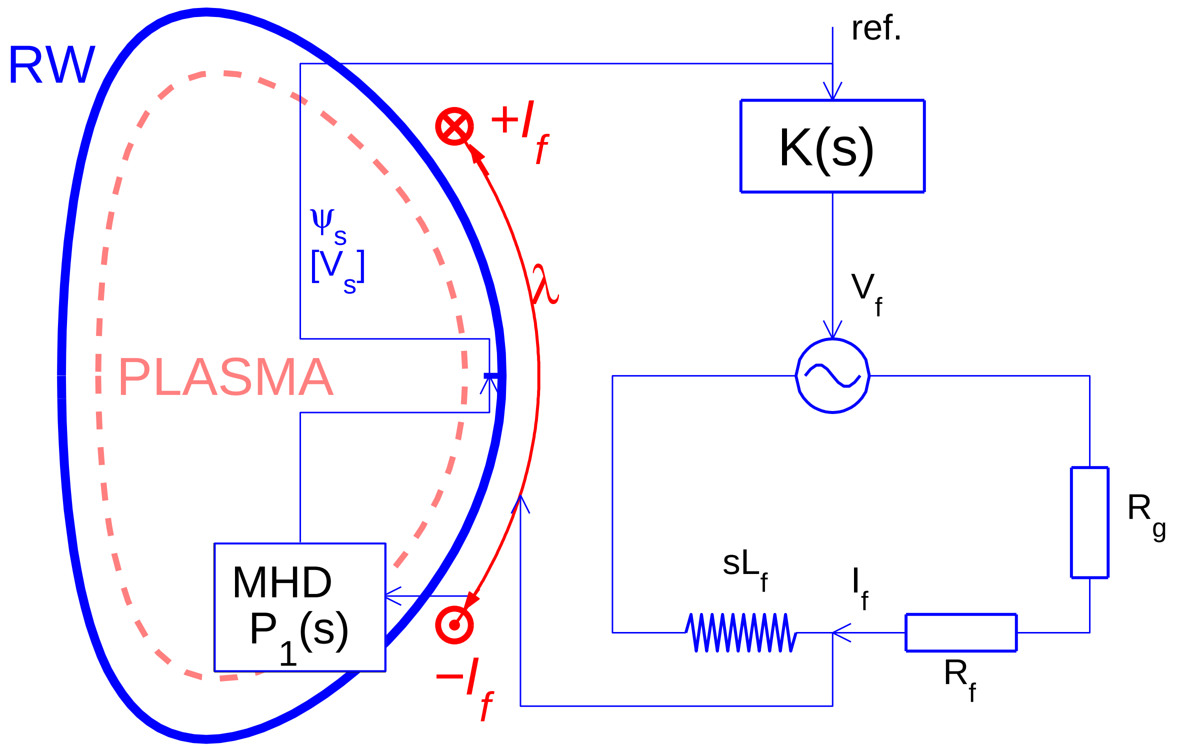


- **Input signal: current $I_f$ or voltage $V_f$**
- **Output signal: flux $\Psi_s$ or voltage $V_s$**
- **Plasma dynamics: $P_1(s)$ – frequency dependent transfer function**
- **$\lambda \equiv$ fraction of poloidal width subtended by active coil**

# RWM control logic

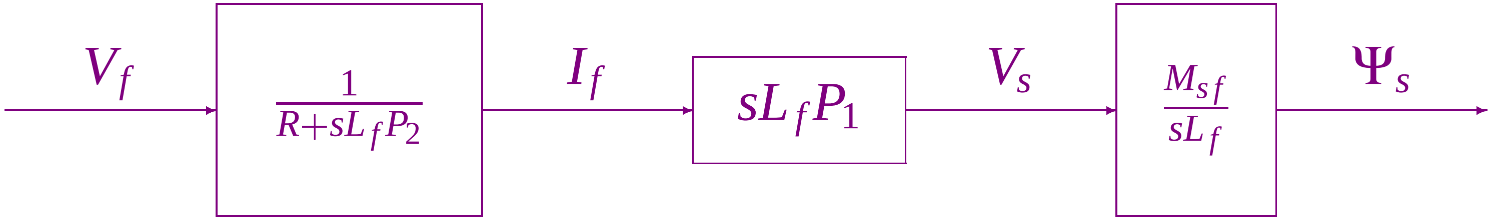


- **Current control:** $I_f = -K\Psi_s/M_{sf}$
  **Frequency response of the plasma-wall system to feedback currents is determined by a non-dimensional transfer function** $P_1(s)$**.**
  **Characteristic equation of closed loop** $1 + K(s)P_1(s) = 0$**.**

- **Voltage control:** $V_f = -KV_s$
  **Introduce non-dimensional transfer function** $P_2(s)$ **for the (normalized) loaded self-inductance of the active coils.**
  **Characteristic equation of closed loop** $1 + K(s)P_1(s)/[P_2(s) + 1/s\tau_f]$**, where** $\tau_f = L_f/R$**.**

- **Plasma response model** $\{P_1(s), P_2(s)\}$ **can be constructed analytically for cylindrical equilibria, and computationally for 2D toroidal hight-**$\beta$ **equilibria using MARS-F code.**

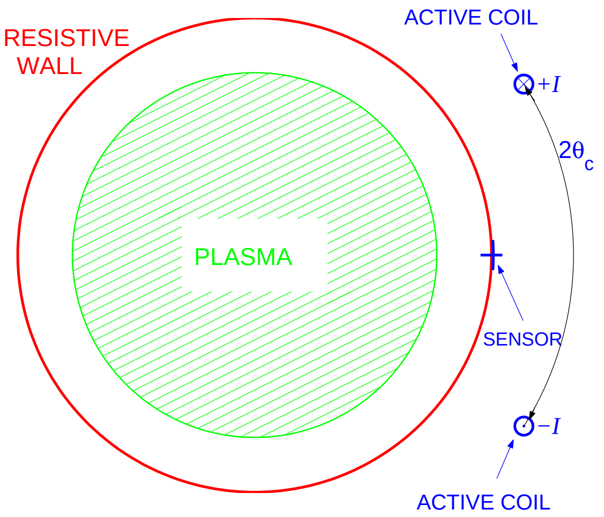


**Representation** $\vec{b} = \nabla\psi \times \hat{z}$

**Stability index** $r_w\psi_m'(r_w^-)/\psi_m(r_w) = -(2\Gamma_m + |m|)$

**Jump at wall** $r_w\Delta_w' = r_w\psi_m'(r_w)|_-^+/\psi_m(r_w) = 2s\tau_w$

**W-o feedback** $\gamma_m\tau_w = \Gamma_m$

**Result** $b_m^{\text{sensor}} = M_m(s) b_m^{\text{coil}} \quad M_m(s) = \dfrac{|m|(r_f/r_w)^{1-|m|}}{s\tau_w - \Gamma_m}$

**Single mode transfer function** $P(s) = M_m(s), \quad b_m^{\text{sensor}} = P(s) b_m^{\text{coil}}$

**Radial or poloidal sensor?** $\{P_m^{(r)}(s), P_m^{(\theta)}(s)\} = \{1, 2\Gamma_m + |m|\} M_m(s)$

**Poloidal sensors superior when $\Gamma \gg 1$, near ideal-wall limit, where $b_r(r_w) = 0$.**

- **Characteristic equation:**

  $1 + K(s)P(s) = 0$, $P = R/(s\tau_w - \Gamma_m)$

- **Nyquist curve:** $K(j\omega)P(j\omega)$, $-\infty < \omega < \infty$ **must encircle -1 in counterclockwise direction.**

- **Single harmonic is easily controlled by proportional current control**

$$1 + K\frac{R}{s\tau_w - \Gamma_m} = 0 \quad \Rightarrow \quad s\tau_w = \Gamma_m - KR$$

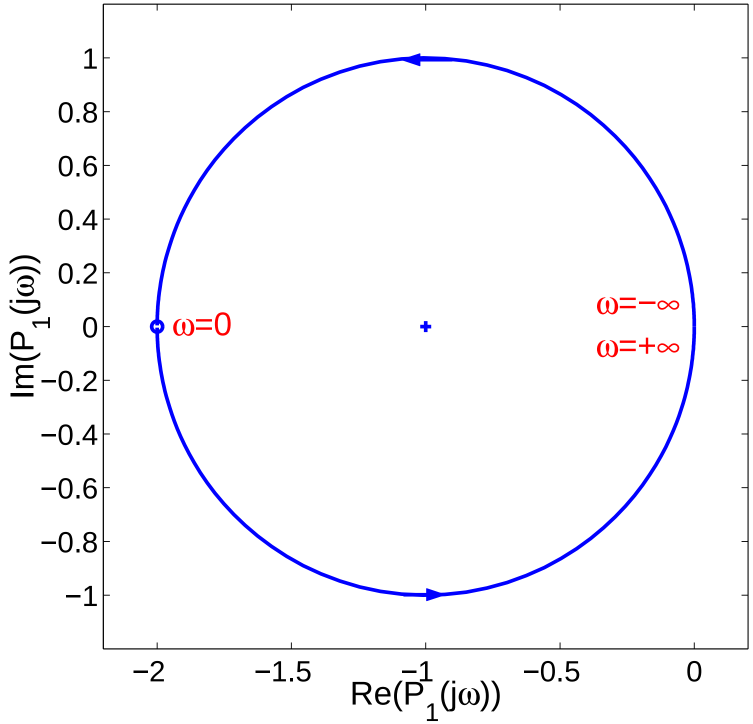


**Feedback works well under single-mode conditions.**

**Decompose antenna current in Fourier components $\Rightarrow$**

**Transfer function** $P^{\{r,p\}}(s) \equiv b_{\{r,p\}\mathrm{sens}}/b_{sf} = \sum_m \{1, (2\Gamma_m + |m|)/m\} M_m(s) c_m$

**where** $M_m(s) = \dfrac{|m|(r_w/r_f)^{|m|-1}}{s\tau_w - \Gamma_m}$, $c_m \propto$ **m-component of active current**

**Poles in $M_m$ correspond to growth-rates for RWM without feedback.**

$P(s)$ **= rational function. Well approximated by low order Padé approximation,** $P(s) = N(s)/D(s)$ **[$N(s)$ quadratic, $D(s)$ cubic].**

# Theory vs. MARS-F computations

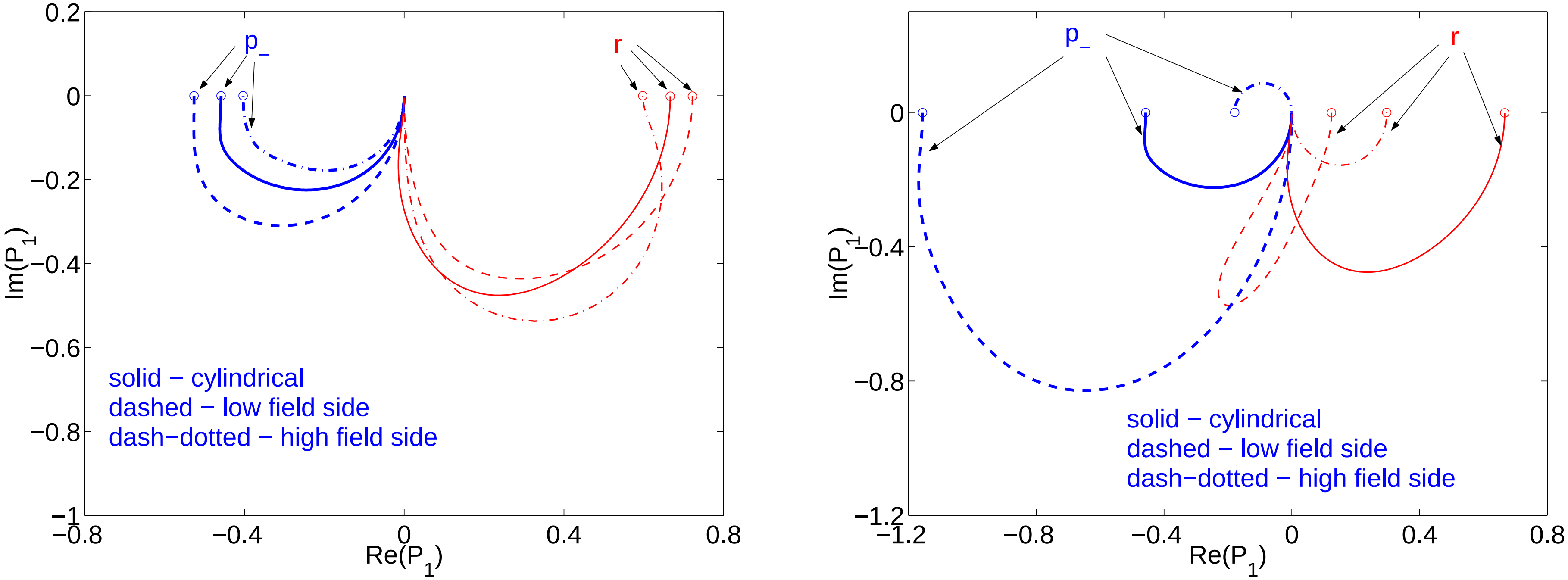


- **MARS-F gives similar transfer functions for (almost) equivalent cylindrical equilibrium ($R/a = 10$)**

- **Toroidal calculations ($R/a \simeq 3$) give more optimistic results than cylindrical theory**
- **Reason: ballooning toroidal mode structure**

# Poloidal vs. radial sensors

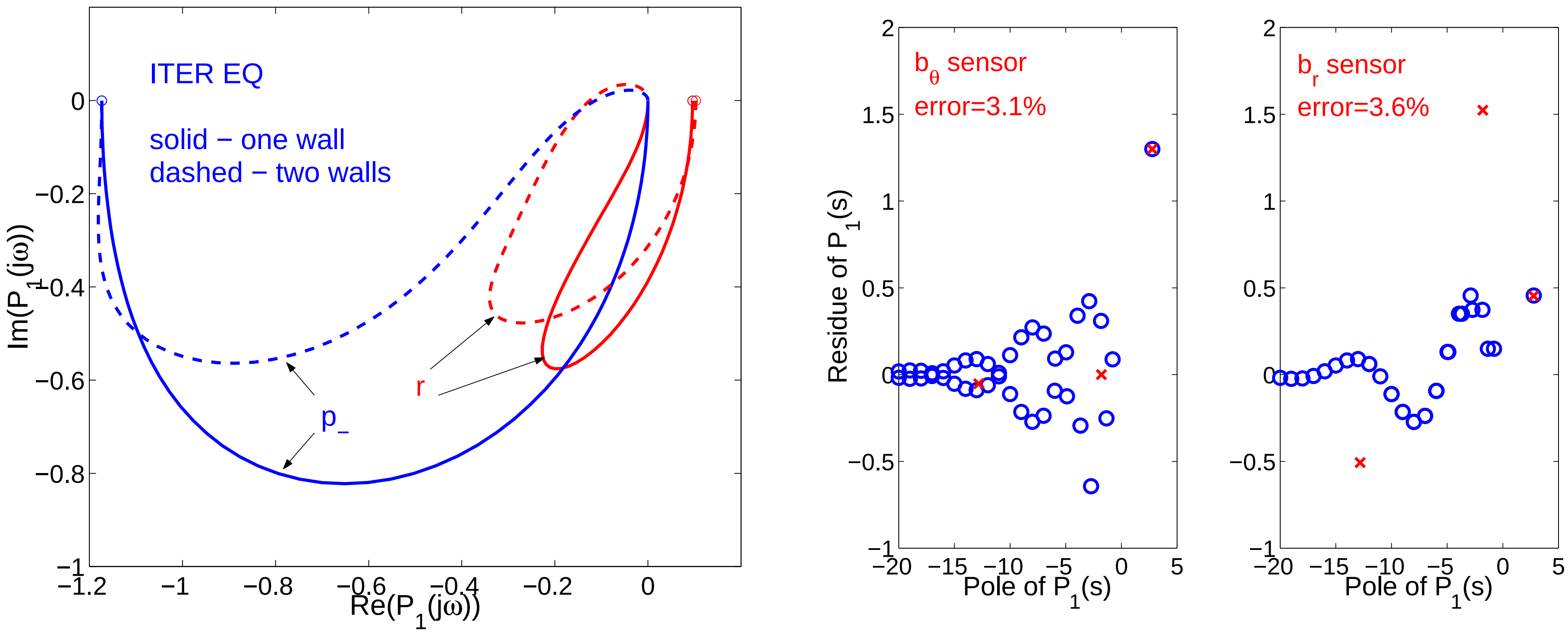


- **Poloidal sensors are superior to radial sensors**
- **Reasons:**
  - **Radial sensors on the wall cannot detect a mode near ideal-wall limit** $\vec{b}\cdot\hat{n}|_{\rm wall}=0$
  - **Poloidal sensors strongly decouple with feedback currents $\Rightarrow$ detect more perturbations from plasma**
  - **Residual cancellation for stable modes $\Rightarrow$ poloidal sensors "see" mostly the unstable mode**

## Performance specifications

- **Sensitivity** $S = 1/(1+KP)$
- **Stability margin:** $J_S = ||S||_\infty = \max_\omega |S(j\omega)| < 2.0$ **keeps system away from marginal stability.**
- **Optimize controller to minimize control activity, e.g, max voltage in initial value problem**

## PID controller for voltage control

$$K_{PID}(s) = \left(K_p + \frac{K_I}{s}\right) \frac{1 + T_d s}{1 + T_d s/\xi}$$

**Control can be made robust w.r.t. plasma pressure, total current, rotation.**

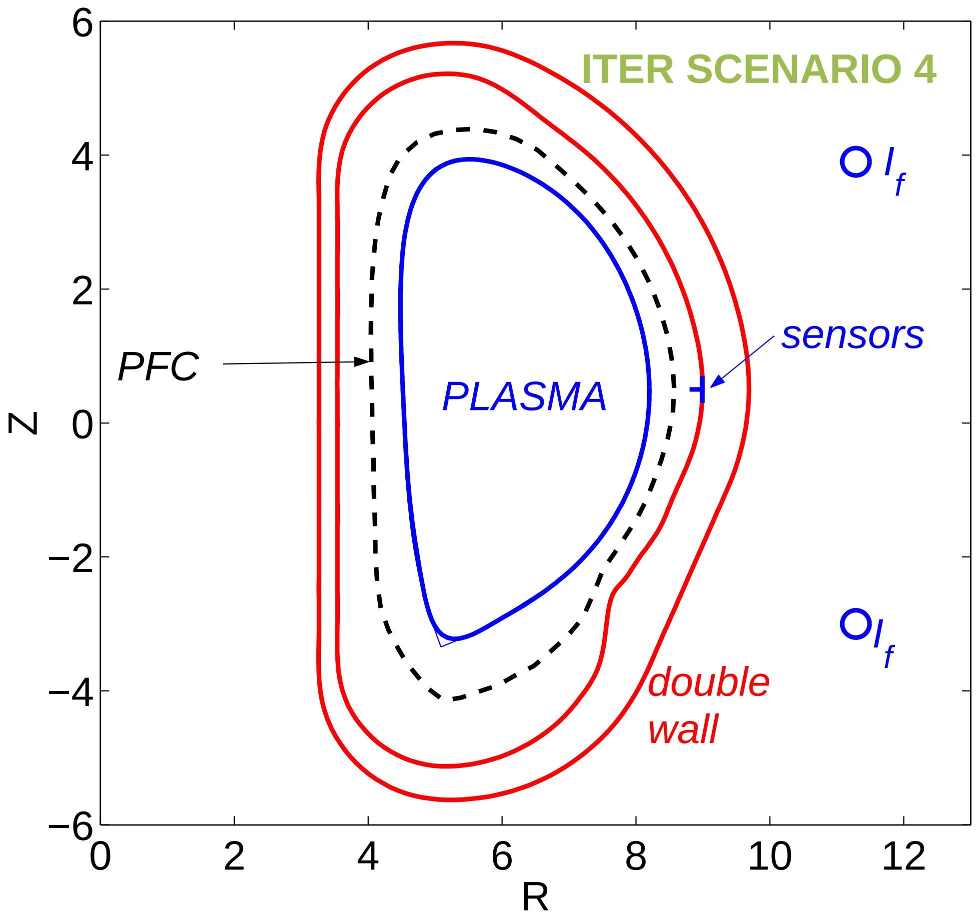


- **EFDA report No. 02-691**
- **Y.Q. Liu, A. Bondeson, Y. Gribov, A. Polevoi, "Stabilization of resistive wall modes in ITER by active feedback and toroidal rotation", to appear in Nucl. Fusion**

- **Both walls and blanket are modeled as continuous, 2D thin shells**
- $\tau_w = 0.188$**s for double wall,** $\tau_b = 9$**ms for blanket**

# RWM control for ITER plasmas

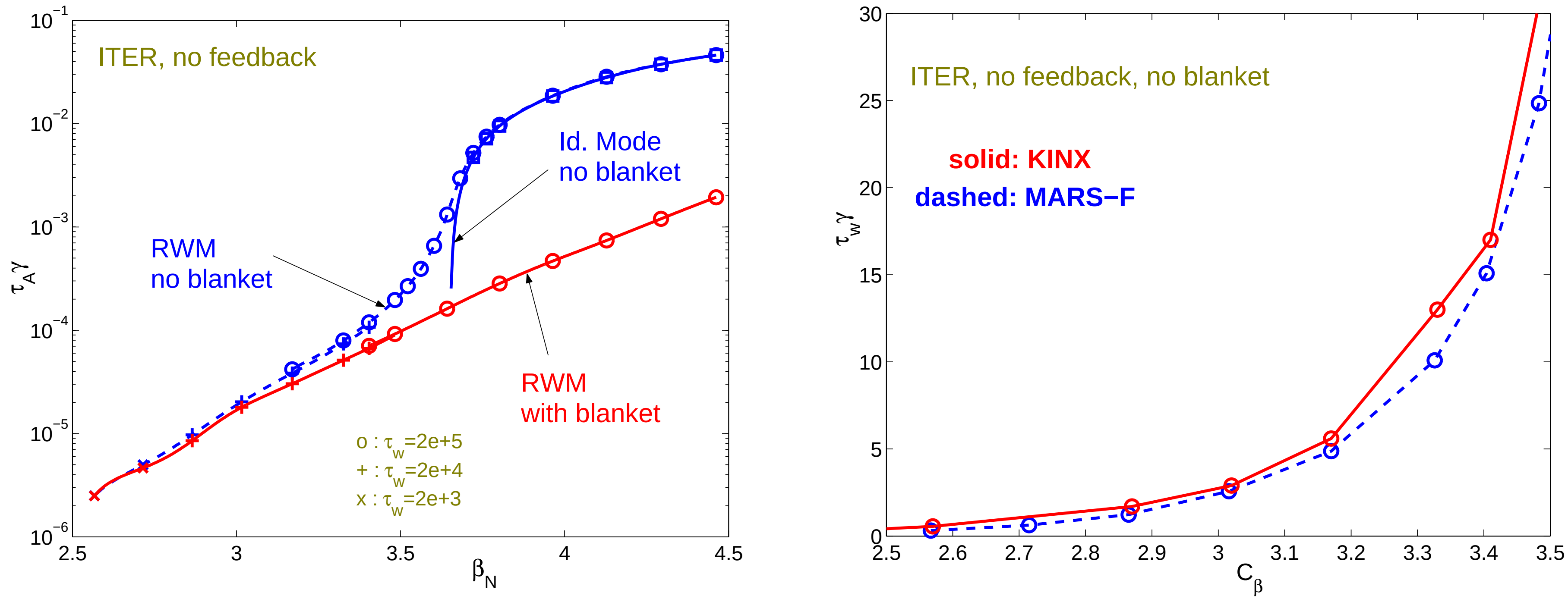


- Growth rates of both ideal kink and RWM show $\beta_N^{\text{ideal-wall}} \simeq 3.65$ without blanket
- Beta limits agree well with KINX and PEST-2
- RWM growth rates agree well with KINX
- Blanket has minor modification to RWM growth rates, as long as $\beta_N$ is not close to ideal wall limit

# RWM control for ITER plasmas

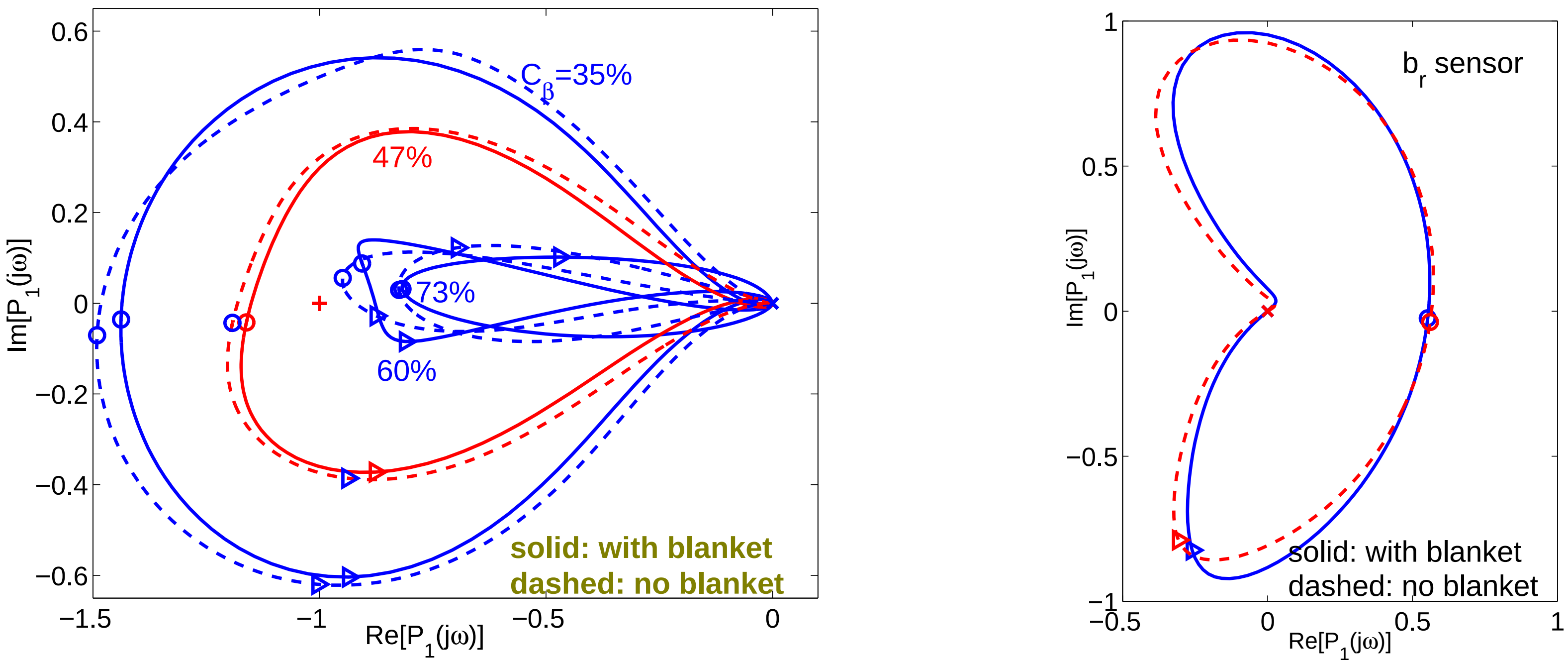


- **With poloidal sensors inside the first wall + proportional control only, RWM can be stabilized up to** $C_\beta \equiv (\beta_N - \beta_N^{\text{no-wall}})/(\beta_N^{\text{ideal-wall}} - \beta_N^{\text{no-wall}}) = 60\%$
- **Adding D-action can stabilize the mode for** $C_\beta \lesssim 70\%$
- **Feedback with radial sensors can not stabilize RWM for** $C_\beta = 47\%$**, with any (stable) PID controller**
- **Blanket modifies only slightly transfer functions**

# RWM control for ITER plasmas

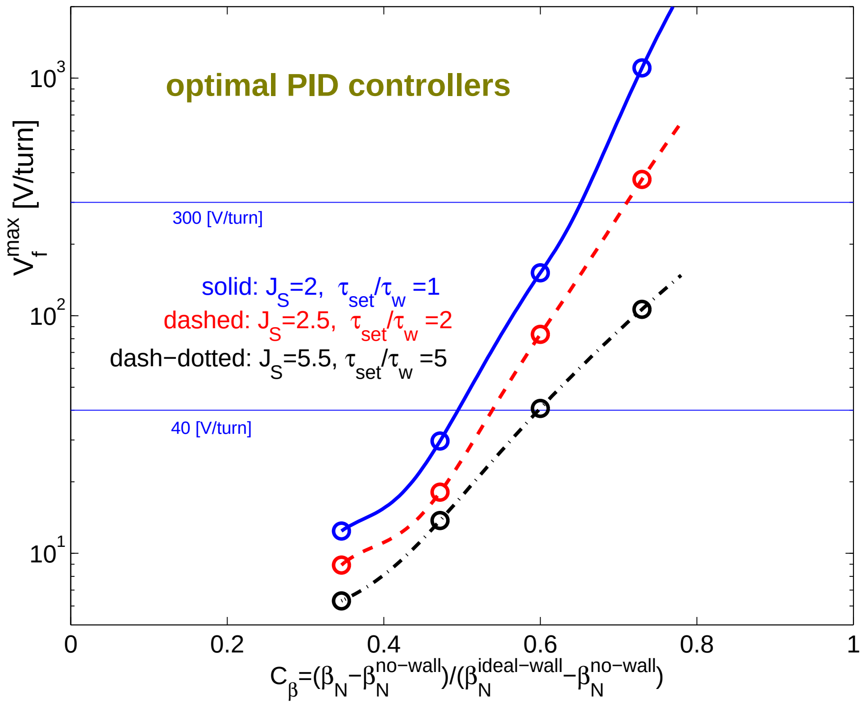


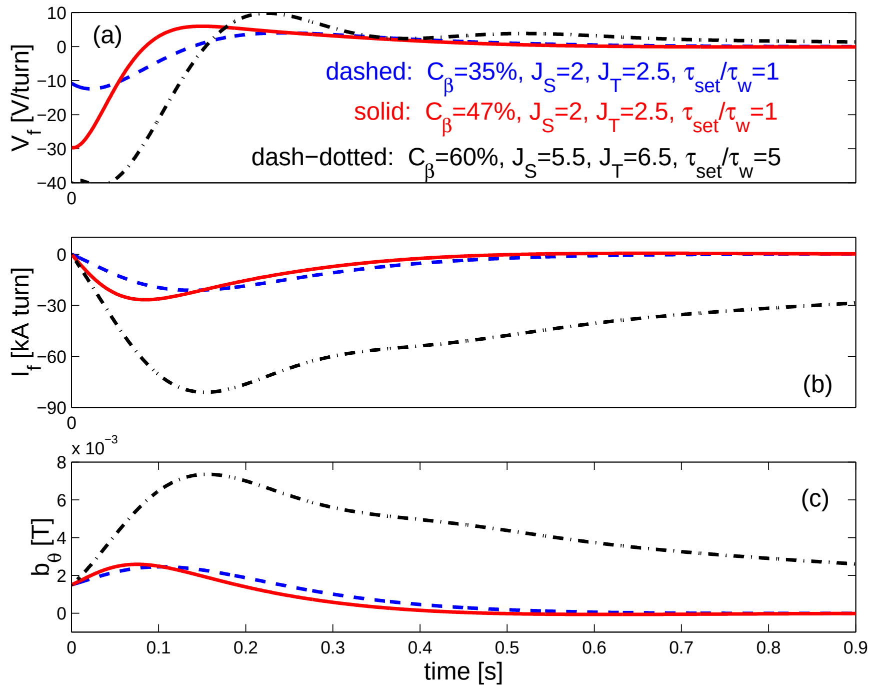


- **Controller optimization made for internal poloidal sensors**
- **With good performance (solid line), RWM can be stabilized up to $C_\beta = 50\%$ if peak voltage limit is 40V/turn, and up to $C_\beta = 60\%$ if voltage limit is 300V/turn**
- **With looser performance (dash-dotted line), RWM can be stabilized up to $C_\beta = 60\%$ if voltage limit is 40V/turn, and up to $C_\beta = 80\%$ if voltage limit is 300V/turn**

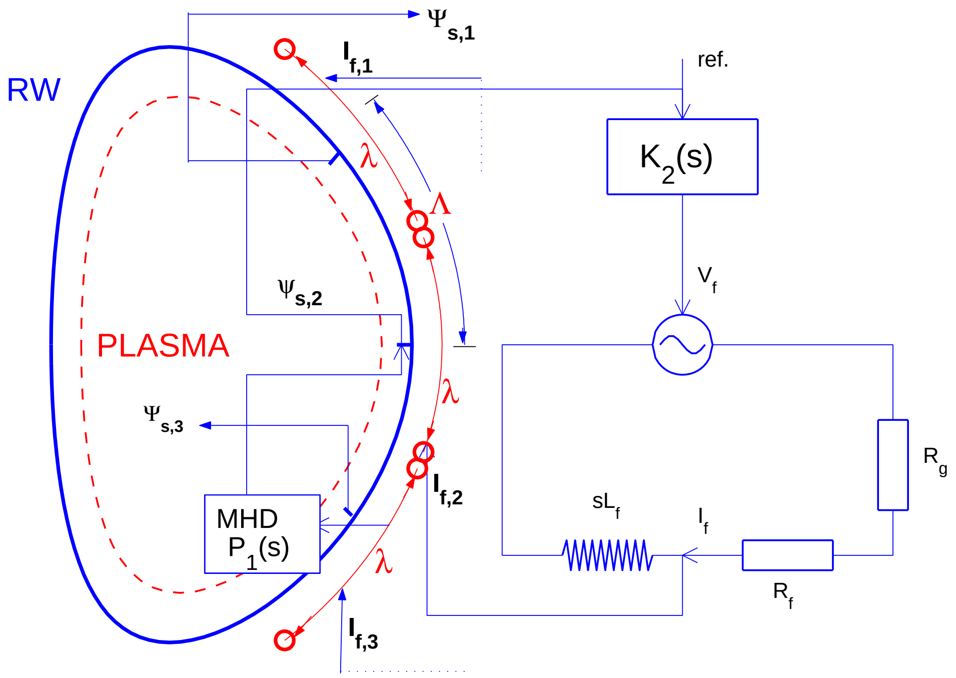


- **MIMO (Multiple Input Multiple Output): each pair of active and sensor coils is connected by an independent controller**
- **MISO (Multiple Input Single Output): all active coils are connected to the same sensor coil by independent controllers**
- $\Lambda \equiv$ **poloidal distance between centers of two neighboring coils**
  $\Lambda > \lambda \rightarrow$ **gap between coils;** $\Lambda < \lambda \rightarrow$ **coils overlap;** $\Lambda = 0 \rightarrow$ **Single Input Single Output**

# Feedback MIMO control - cylindrical theory

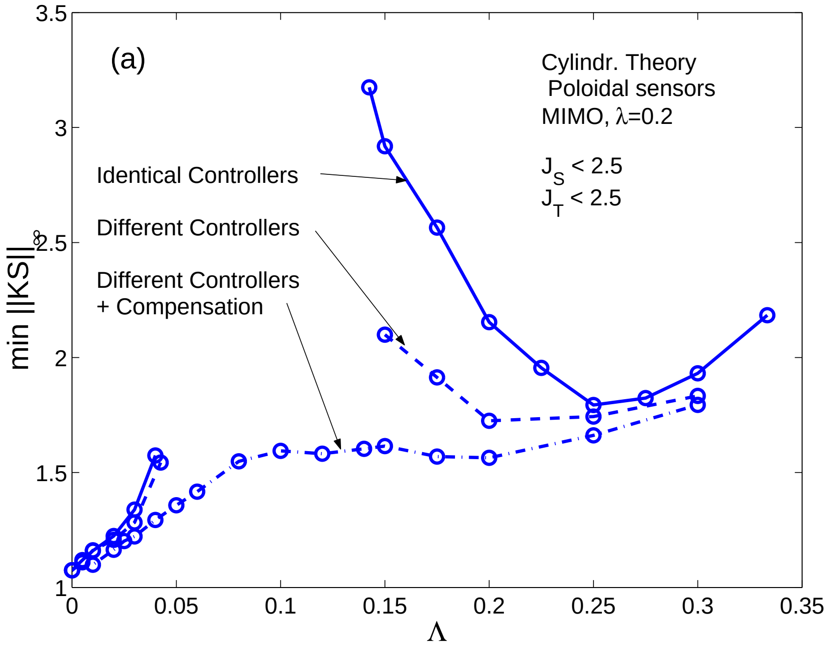


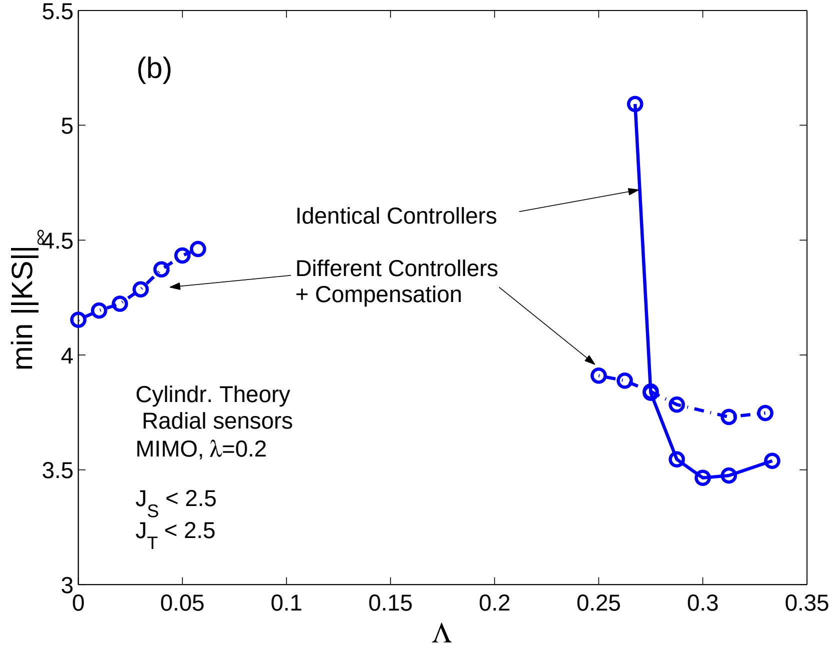


- **With poloidal sensors, single coil ($\Lambda = 0$) works better than multiple coils ($\Lambda > 0$) in terms of control activity.**
- **With radial sensors, MIMO system improves feedback control. Good results are obtained when three active coils are well separated ($\Lambda > \lambda$) $\Longrightarrow$ reduced coil coupling.**

## MIMO control - toroidal computations

| | sensor | ctrl. | $J_S$ | $J_T$ | $J_u$ |
|---|---|---|---|---|---|
| SISO | pol. | single | 1.00 | 1.73 | 0.98 |
| MIMO | pol. | identic. | 2.11 | 2.50 | 1.32 |
| MIMO | pol. | diff. | 1.36 | 1.92 | 0.69 |
| SISO | rad. | single | 1.37 | 1.68 | 3.65 |
| MIMO | rad. | identic. | 1.46 | 1.59 | 24.7 |
| MIMO | rad. | diff. | 1.87 | 2.10 | 3.48 |

- For both types of sensors, MIMO with identical controllers gives worse results than SISO, in terms of control activity $J_u = ||KS||_\infty$
- MIMO with different controllers (in diagonal controller matrix) gives comparable results to SISO
- Results for a JET shaped advanced equilibrium, more study with DIII-D plasmas expected

- MARS-F is now used at General Atomics (M.S. Chu et al. APS DPP03 invited talk)

**Theory for cylindrical tokamak:** $\vec{b} = \nabla\Psi \times \hat{z},\ \Psi = \psi_m(r)\exp(jm\theta - jn\phi)$

- **The stability of the RWM is determined by**

$$r_w \Delta'_w \equiv r_w \frac{\psi'_m(r_w^+) - \psi'_m(r_w^-)}{\psi_m(r_w)} = 2\gamma\tau_w$$

- **RWM growth rate $\gamma = O(1/\tau_w) \ll \omega_0$ = plasma rotation frequency, so $\gamma \simeq 0$ is a good approximation inside the plasma.**
- **Resonances at $\omega_0 = \pm k_{\|} v_A = \pm\omega_A(x)$ near rational surfaces.**
- **"Resonance layer problem" has external asymptotes for $|x| \gg |\omega_0/\omega'_A|$**

$$\psi(x) = c_1\left(-j\pi|x| + \frac{2\omega_0}{|\omega'_A|}\right) + c_2 x$$

- **Internal delta-prime: $\Delta'_{\mathrm{int}} = -j\pi|\omega'_A|/\omega_0$ (independent of $\gamma$)**

- $\psi_0(r) =$ **no-wall solution and** $\psi_\infty(r) =$ **ideal-wall solution.**
- **Matching at wall gives** $\psi(r) = \psi_0(r) + \gamma\tau_w\psi_\infty(r)$
- **Set** $\psi_{\{0,\infty\}} = \psi_{\{0,\infty\}}(r_s)$ **and** $\delta_{\{0,\infty\}} = \psi'_{\{0,\infty\}}(r_s^+) - \psi'_{\{0,\infty\}}(r_s^-)$. **External delta-prime is**

$$\Delta'_{\text{ext}} = \frac{\delta_0 + \gamma\tau_w\delta_\infty}{\psi_0 + \gamma\tau_w\psi_\infty}$$

- $\Delta'_{\text{ext}} = \Delta'_{\text{int}}$ **gives**

$$\gamma\tau_w = -\frac{|\omega'_A|\psi_0 - \delta_0 j\pi\omega_0}{|\omega'_A|\psi_\infty - \delta_\infty j\pi\omega_0}$$

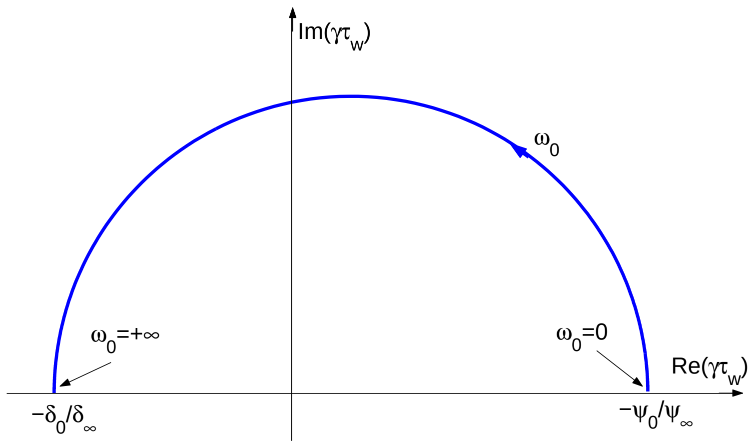


- **Wall stabilized case:** $\psi_0 < 0$, **and** $\psi_\infty, \delta_0, \delta_\infty > 0$
- **RWM rotates in the direction of plasma flow**
- **RWM rotation** $\to 0$ **as** $\omega_0 \to 0, \infty$
- **Required** $\omega_0$ **for stability** $\to 0$ **near ideal-wall marginal point** $\psi_\infty \to 0$.

# Ion Landau damping

- Toroidal ideal-MHD predictions for critical rotation velocity $> 0.02v_A$ in $q \sim 2$ region
- Ideal-MHD threshold is generally some fraction higher than experimental results (Garofalo, et al 2002). Example: 50% higher than experiment for DIII-D discharge 92544.
- Predicted critical rotation decreases if extra drag mechanism is introduced.
- Good candidate - ion Landau damping.
- Previously modeled in MARS as a parallel viscosity (parallel sound wave damping model)

$$\vec{F}_{\mathrm{visc}} = -\kappa_{\|} |k_{\|}| v_{th,i} \rho \vec{v}_{\|}$$

- Drift-kinetic analysis showed reduced damping by $\sim (v_\phi / v_s)^6 (R/a)^3$. What $\kappa_{\|}$ to use?
- New approach - use kinetic large-aspect-ratio theory to approximate dissipative terms.
- Semikinetic damping model gives lower critical rotation and reproduces error field amplification experiments.

- **Follow simplified drift-kinetic large-aspect-ratio analysis (Bondeson & Chu 1996)**
- **Take imaginary part of kinetic $\Delta W$ evaluated for $\omega = \omega_0$ and add as a force acting on $\vec{v}_\perp$:**

$$
\begin{aligned}
j\mathrm{Im}(\Delta W_C + \Delta W_T) &= -\frac{1}{2}\int \vec{F}_{\mathrm{diss}} \cdot \vec{\xi}_\perp^{\,*} d^3x, \quad H = \mu Q_L + m v_{||}^2 \vec{\xi} \cdot \vec{\kappa} \\
\Delta W_T &= \frac{1}{2}\sum_{m'} \int d^3x \int_{trapped} d\Gamma \left(-\frac{\partial f}{\partial E}\right) \frac{\omega}{\omega + m'\omega_b} |< \exp(j\chi_{m'}) H > |^2 \\
\Delta W_C &= \frac{1}{2}\sum_{m'} \int d^3x \int_{circ} d\Gamma \left(-\frac{\partial f}{\partial E}\right) \frac{\omega}{\omega - (nq - m')\omega_t} |< \exp(j\chi_{m'}) H > |^2
\end{aligned}
$$

- **Toroidal coupling: $m$ component of $\vec{b}$ couples to $m \pm 1$ components of parallel motion.**
- **Strong kinetic damping even at low rotation: $m = 2$ component of $\vec{b}$ couples to $m = 1,3$ components of $\vec{v}_{||}$ which has thermal phase velocity close to $q = 1,3$.**
- **Landau damping is very nonlocal. Even at $\omega_0 \sim 0.02\omega_A$ momentum transfer is spread out over entire plasma.**

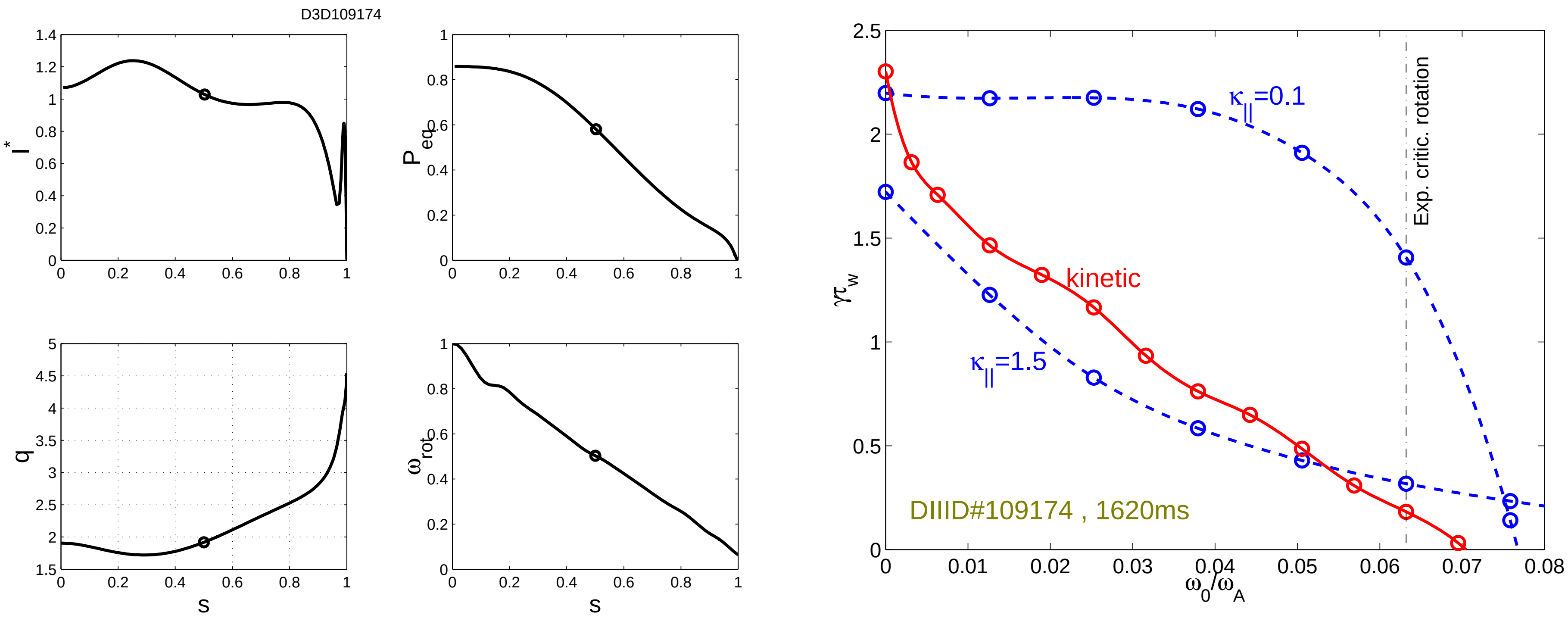


Experimental data from R. La Haye

- **Kinetic damping model gives good prediction of critical rotation speed.**
- **Parallel sound wave damping model with small $\kappa_{||}$ also works, but large $\kappa_{||}$ somewhat fails.**
- **For many other equilibria, larger $\kappa_{||}$ is more stabilizing!**

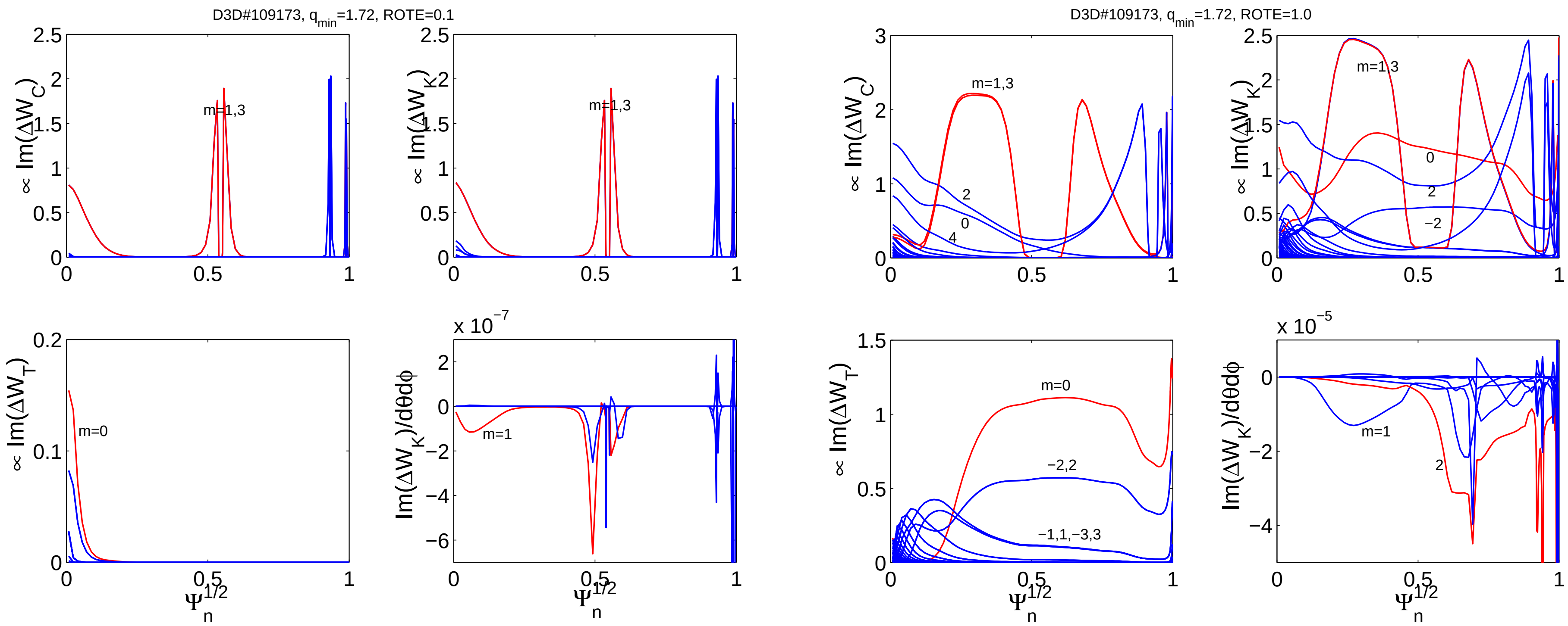


- **Slow rotation** $\omega_{\mathrm{rot}}/\omega_{\mathrm{exp}} = 0.1$
- **Fast rotation** $\omega_{\mathrm{rot}}/\omega_{\mathrm{exp}} = 1.0$
- **At fast rotation, kinetic damping is strong around regions** $q \sim 2$**, and quite global**
- $m = 2$ **component of** $\vec{b}$ **drives** $m = 1, 3$ **components of** $\vec{v}_{||}$

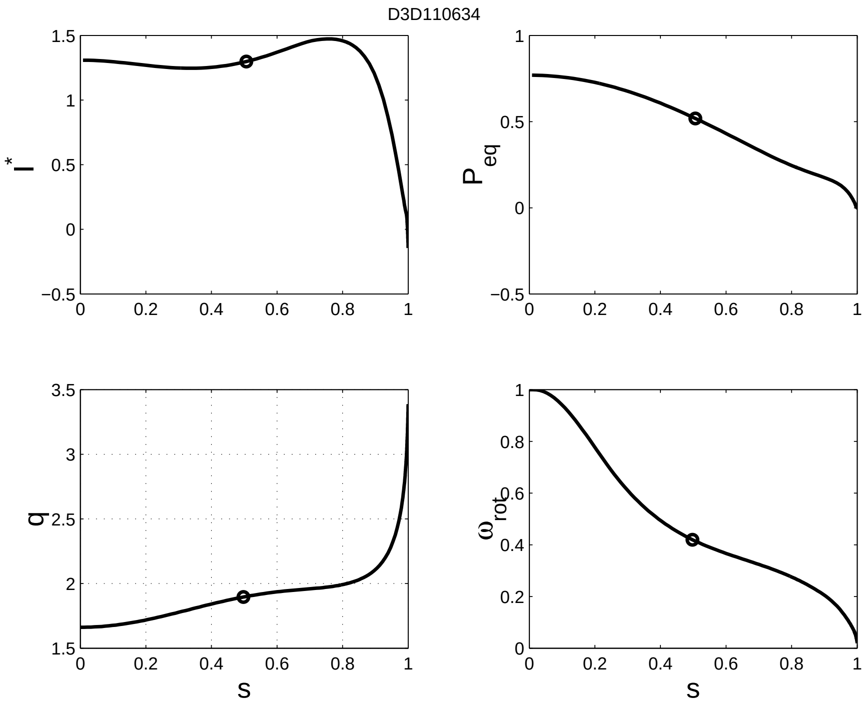


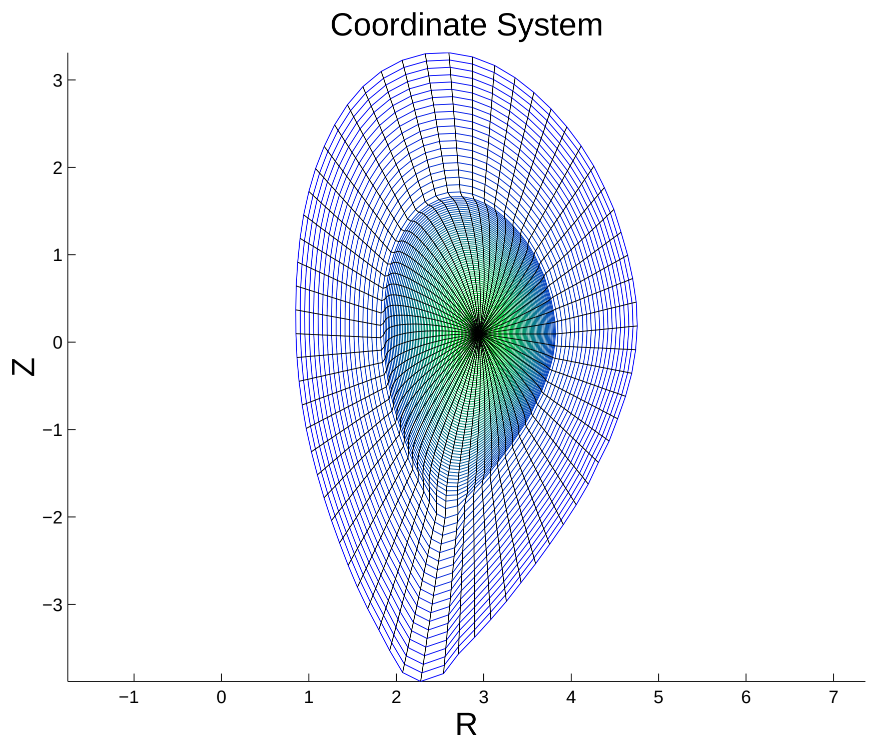


**Experimental data from A. Garofalo**

- **Discharge with low** $q_{95} \simeq 2.52$
- **Experiments: rotational stabilization becomes more difficult with decreasing** $q_{95}$

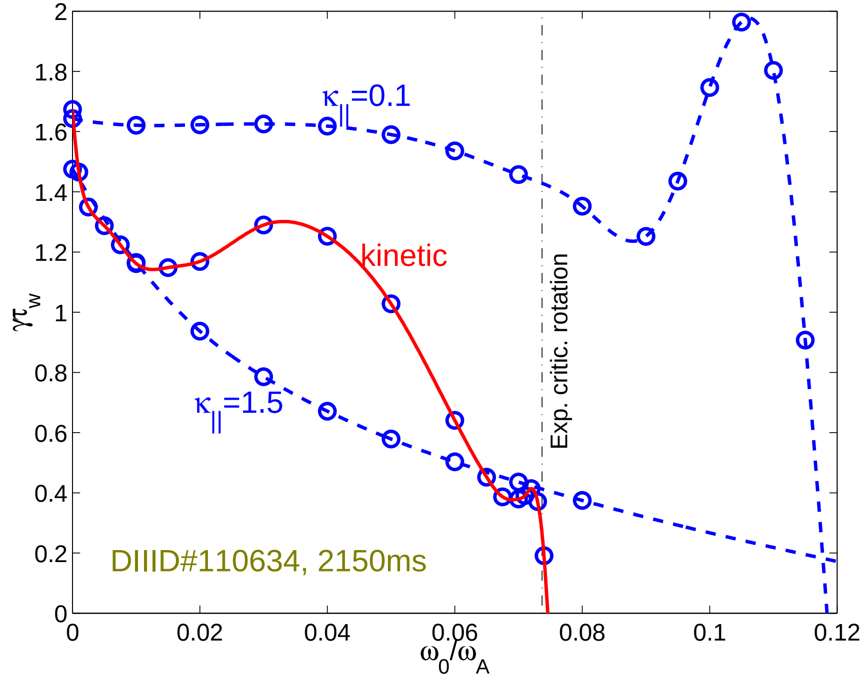


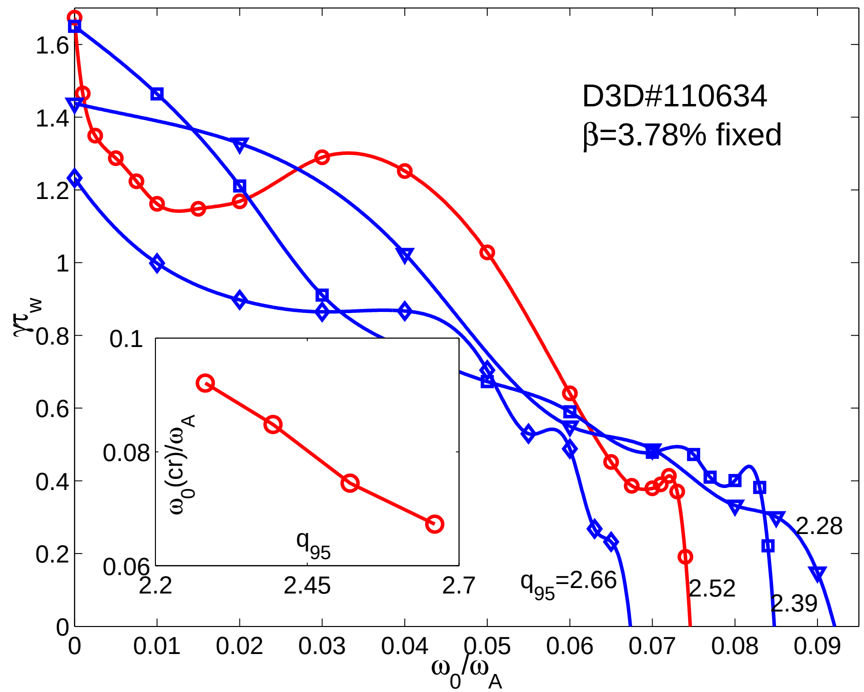


- **Kinetic model predicts stabilization at experimental rotation frequency at $t = 2150$ms**
- **Scanning $q_{95}$, with fixed $\beta = 3.78\%$, gives correct trend**

# ITER steady state Scenario-4

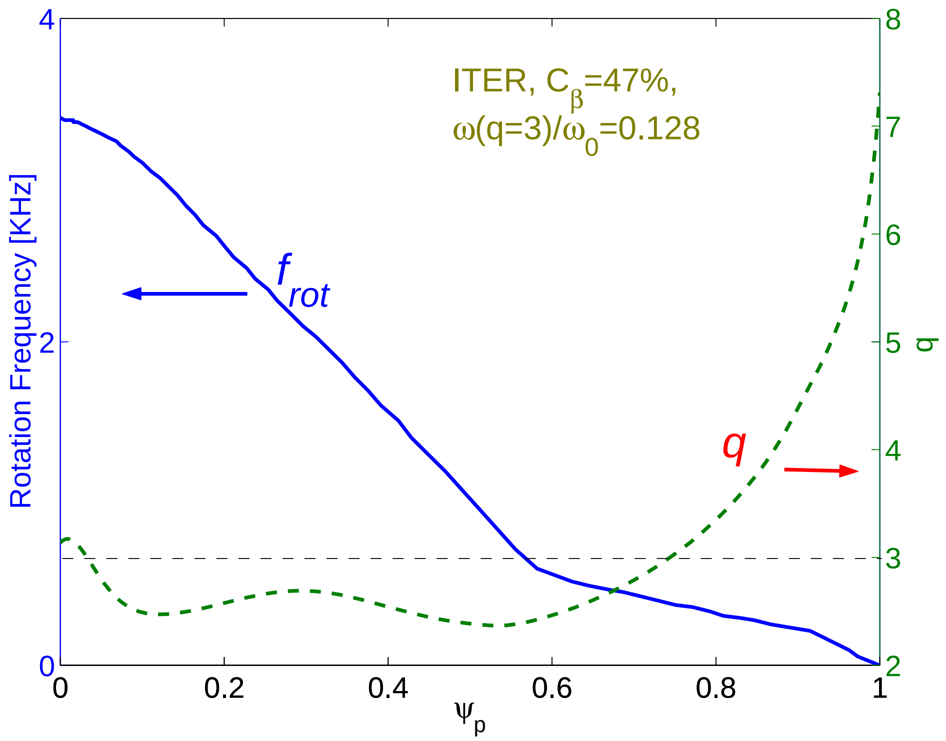


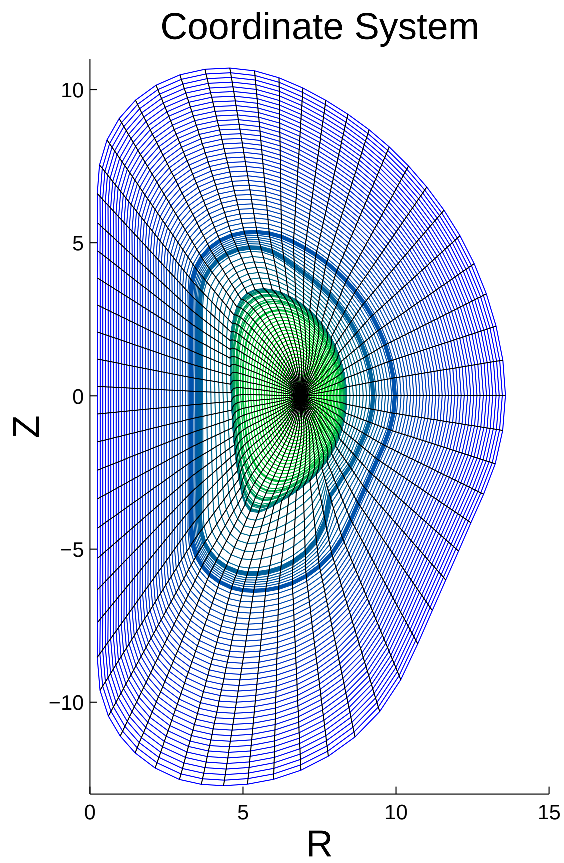


- $R_0 = 6.35m, \quad a = 1.85m, \quad I_p = 9\mathrm{MA}, \quad Q = 5$
- **Highly shaped plasma:** $\kappa_{\mathrm{sep}} = 1.97, \quad \delta_{\mathrm{sep}} = 0.58$
- **Design:** $\beta_N = 2.57$
- **MARS:** $\beta_N^{\mathrm{no-wall}} \simeq 2.45, \quad \beta_N^{\mathrm{ideal-wall}} \simeq 3.65$

# Rotation ITER steady state Scenario-4

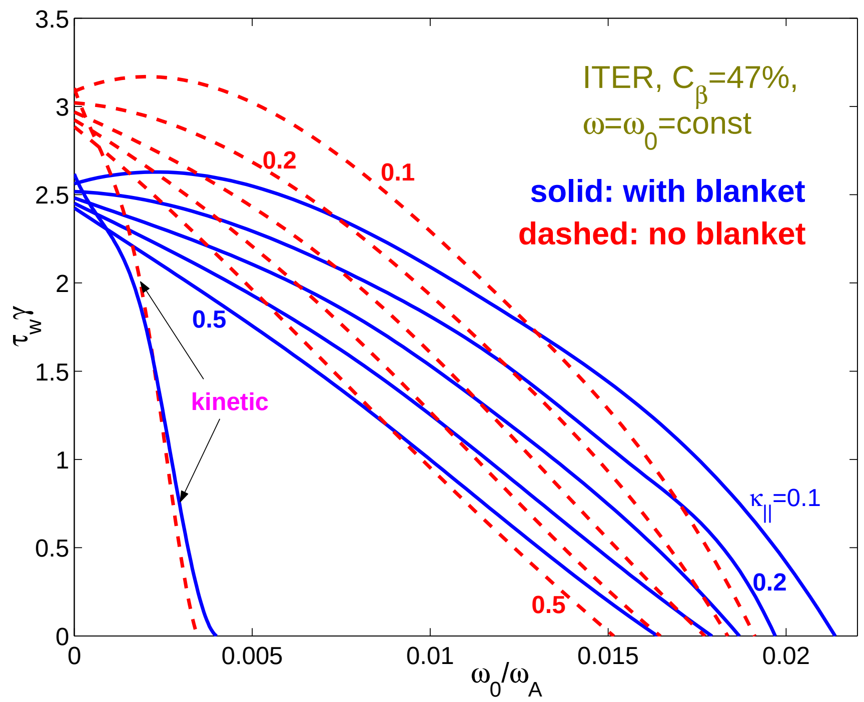


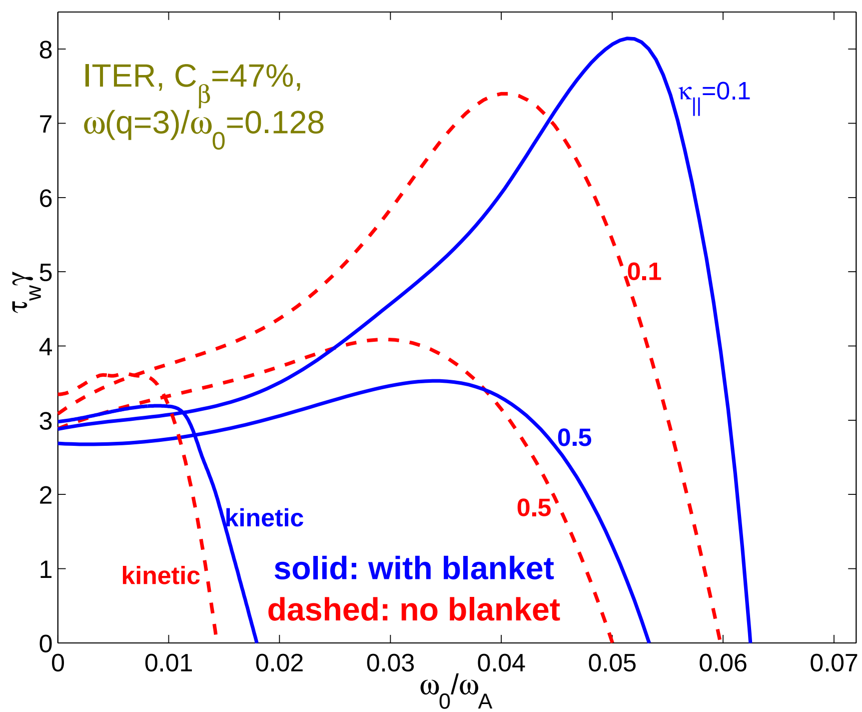


- **With uniform rotation profile, parallel damping model predicts critical central rotation frequency $\lesssim 2\%\omega_A$; kinetic damping gives $\lesssim 0.5\%\omega_A$**
- **With predicted rotation profile, parallel damping model gives critical rotation at about $5-6\%\omega_A$; kinetic model gives $\lesssim 2\%\omega_A$**
- **Predicted ITER central rotation frequency is about $2\%\omega_A$**
- **Generally, blanket slightly increases critical rotation**

**Single mode:**

$$\psi = \psi_p \left(\frac{r}{r_w}\right)^{-m} + \psi_w \begin{cases} \left(\frac{r}{r_w}\right)^{m}, & r \le r_w \\ \left(\frac{r}{r_w}\right)^{-m}, & r > r_w \end{cases} + \psi_f \begin{cases} \left(\frac{r}{r_f}\right)^{m}, & r \le r_f \\ \left(\frac{r}{r_f}\right)^{-m}, & r > r_f \end{cases}$$

$$\frac{\psi'_{r=a+}}{\psi_{r=a}} = -\frac{m}{a}(1 + x + jy)$$

$$\gamma\tau_w = r_w \Delta'_w = r_w \frac{\psi'_{r_w+} - \psi'_{r_w-}}{\psi_{r_w}}$$

$\psi_f = -K \cdot r_w \psi'_{r_w-}$ **(internal poloidal sensor)**

$$\Longrightarrow \quad P_1^{\theta} = \left(\frac{r_w}{r_f}\right)^{m} \frac{2m}{s - s_0}\left(\frac{2}{H} - 1\right), \quad s_0 = 2m\left(\frac{1}{H} - 1\right), \quad H = 1 - \frac{x + jy}{2 + x + jy}\left(\frac{r_w}{a}\right)^{2m}$$

**Single mode cylindrical model**

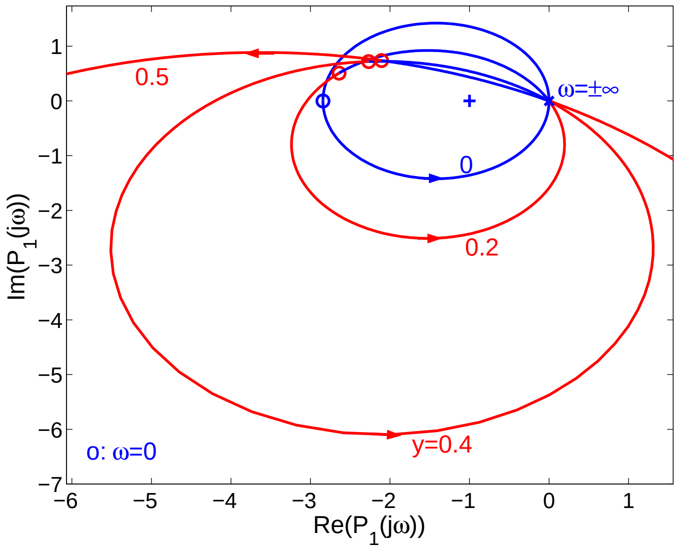


**Toroidal computation by MARS**

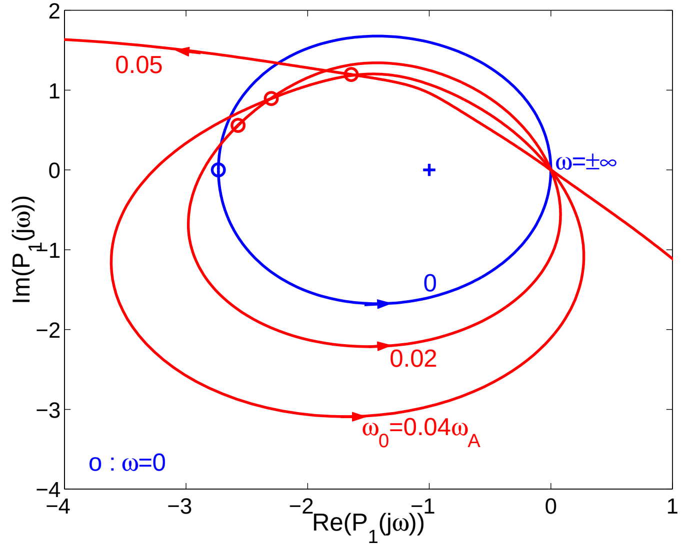


- **Phase of optimized controller gain corresponds to rotation direction, increases with increasing rotation frequency**
- **For ITER plasma, when performance constraint ($J_S$) is not very strict, rotation helps feedback, in terms of required peak voltage for feedback coils**

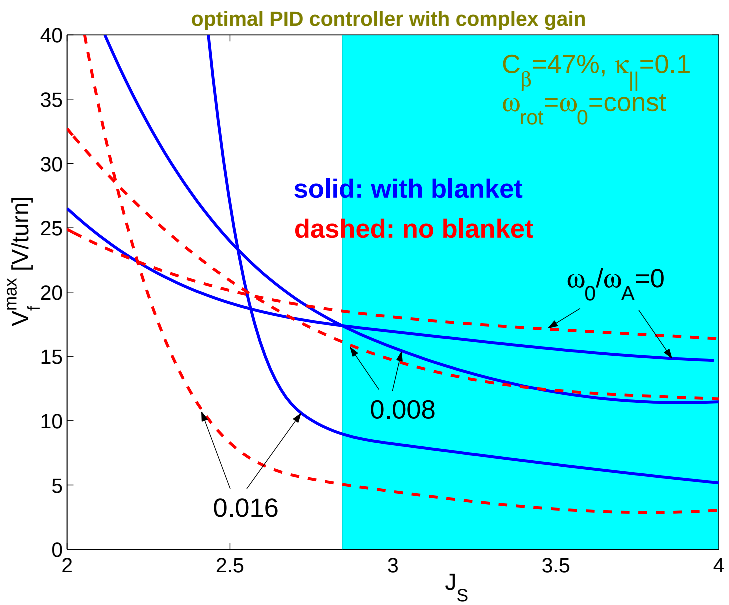

# JET #59223 - static error field

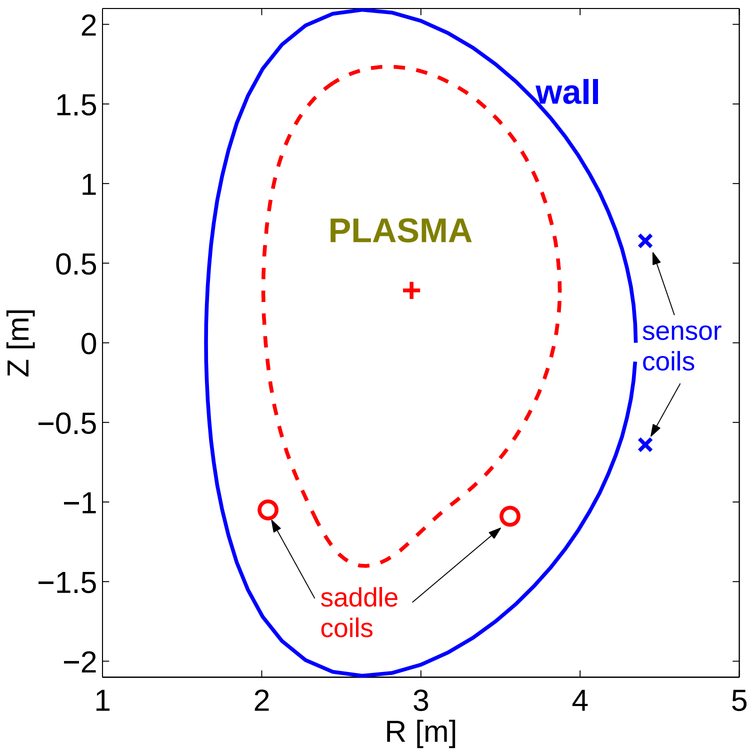


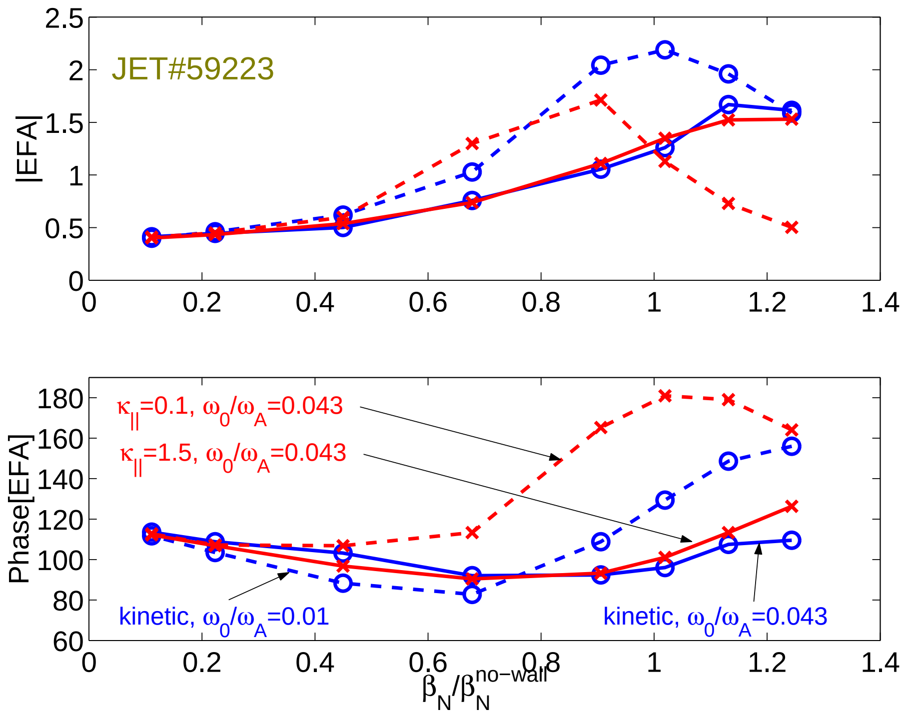


**Experimental data from T. Hender**

- **Weak parallel sound wave damping does not reproduce experimental behavior of (static) error field amplification**
- **Strong parallel sound wave damping or kinetic damping model works well**
- **Kinetic damping model has no free parameter!**
- **RFA serves good tool to test different damping models**

# EFA increases with β - no sharp threshold at no wall limit

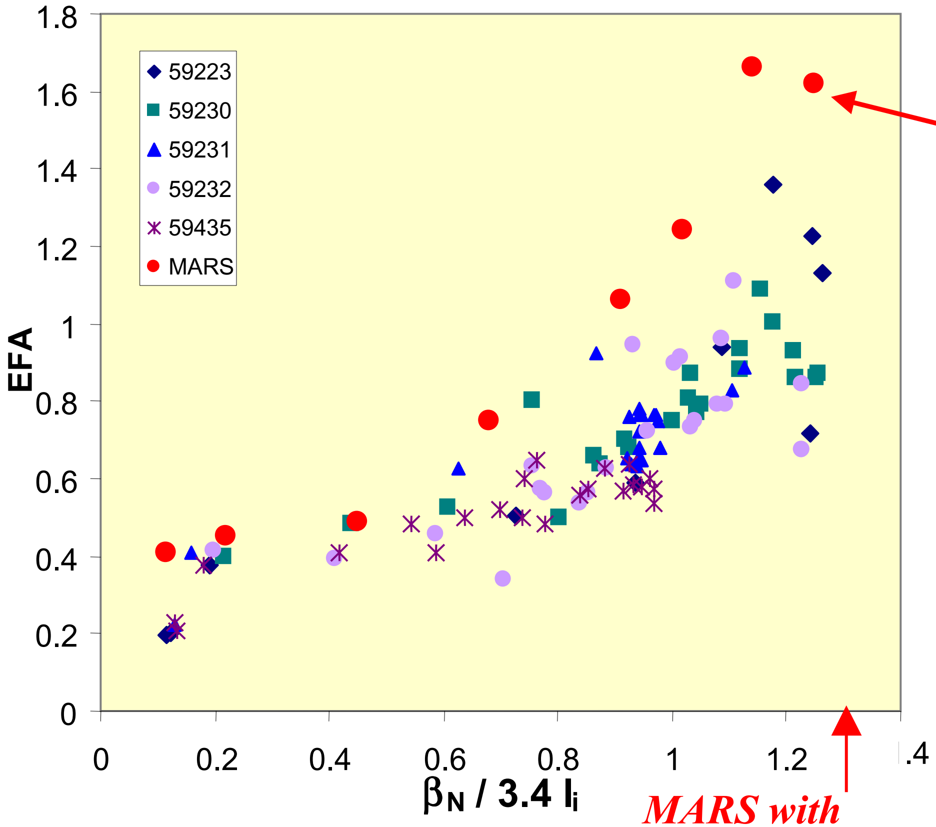


*MARS code results including kinetic damping model - no free parameters.*

*MARS with wall beta limit*

# Phase also agrees well MARS simulation

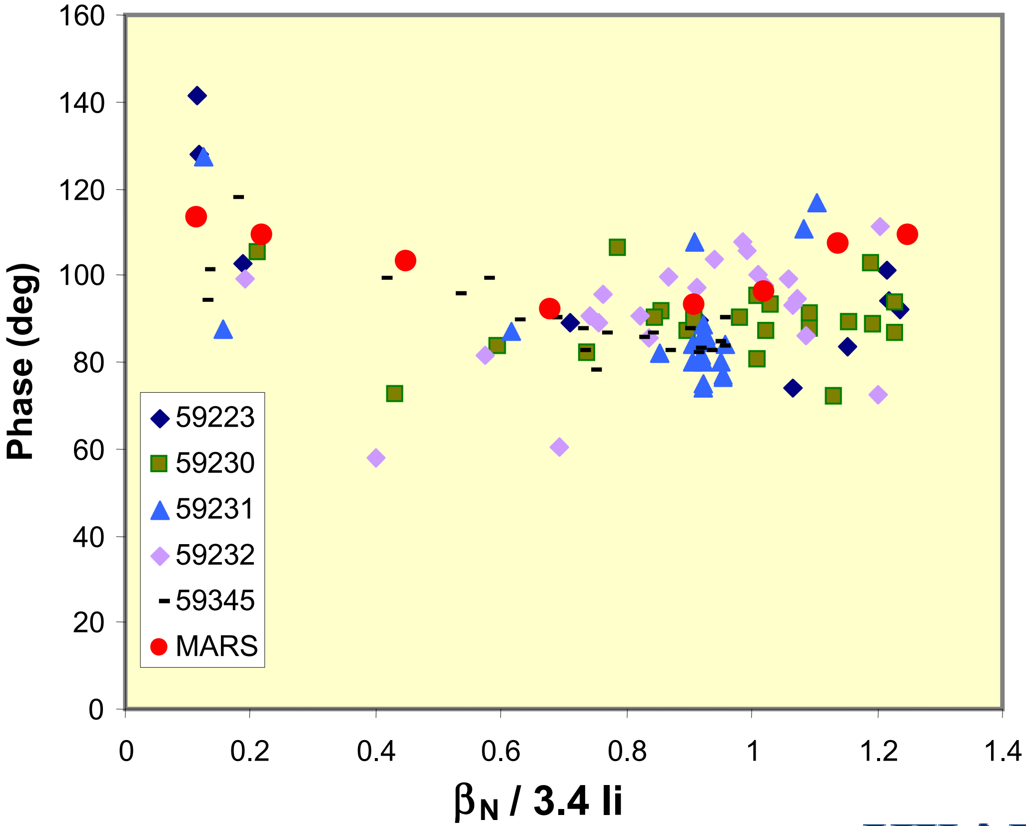

# JET #59223 - Time-varying error field

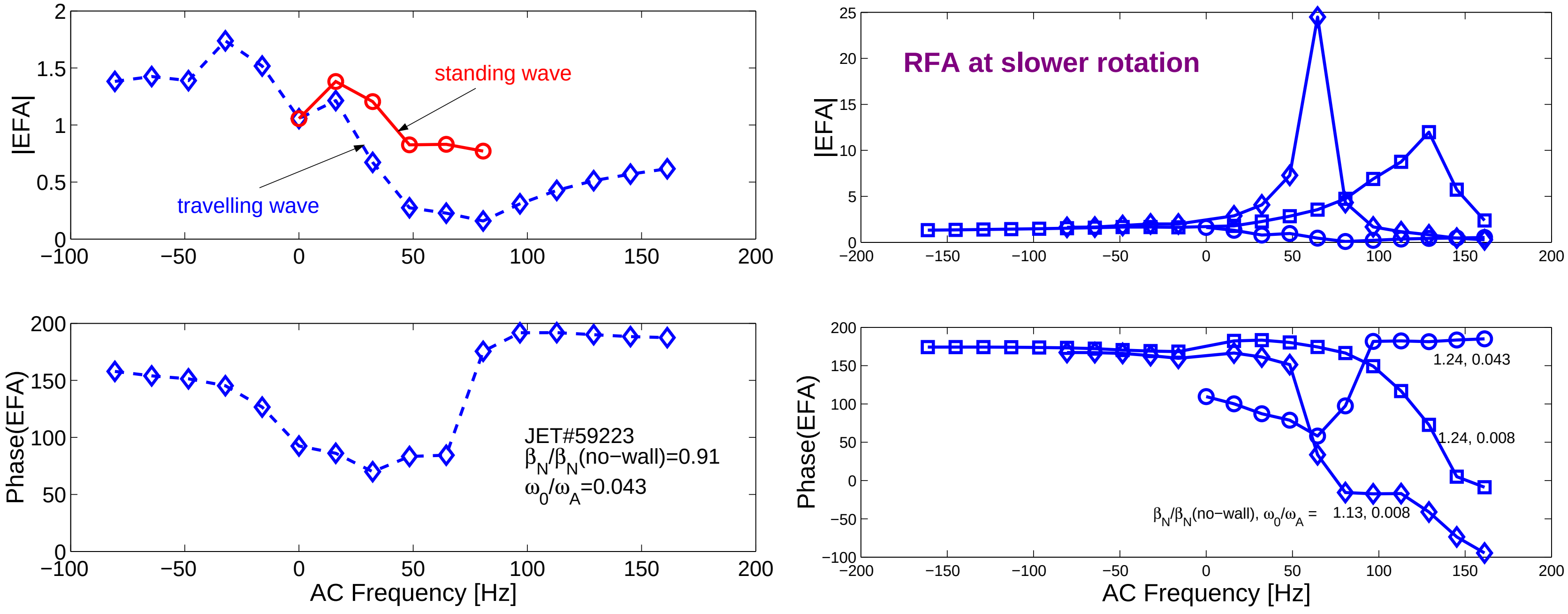


- **No clear resonant effect at experimental plasma rotation speed**
- **Clear resonant effect should be seen at slowed-down rotation**

## Conclusions

- $n = 1$ **RWM can be feedback controlled for** $\beta$ **up to** $\beta^{\text{no wall}} + C_\beta(\beta^{\text{ideal wall}} - \beta^{\text{no wall}})$ **with** $C_\beta \sim 0.6 - 0.8$, **by**
  - **single feedback coil outside the resistive wall**
  - **poloidal sensors inside the vessel**
  - **PID controller**
- **Ideal MHD theory, with adequate choice of damping mechanisms, gives reasonable prediction of rotational stabilization of RWM.**
- **RFA can be very useful to distinguish different damping models for RWM in a rotating plasma.**
- **Damping models involving strong damping give better prediction of the critical rotation speed and RFA. Kinetic model without free parameter usually agrees with experiment.**
- **Synergy between rotation and feedback occurs as long as rotation stabilizes RWM.**